Deciphering the proteomic signatures of the optic nerve glial lamina in healthy and glaucomatous conditions

by
Zollie Yavarow

Department of Pharmacology and Cancer Biology
Duke University

Date:_____

Approved:

_____
Romain Cartoni, Supervisor

_____
Nina Tsvetanova

_____
Vadim Arshavsky

_____
Debby Silver

_____
Beth Sullivan

Dissertation submitted in partial fulfillment of
the requirements for the degree of Doctor of Philosophy in the Department of
Pharmacology and Cancer Biology in the Graduate School
of Duke University

2022

ABSTRACT

Deciphering the proteomic signatures of the optic nerve glial lamina in healthy and glaucomatous conditions

by
Zollie Yavarow

Department of Pharmacology and Cancer Biology
Duke University

Date:_____

Approved:

_____
Romain Cartoni, Supervisor

_____
Nina Tsvetanova

_____
Vadim Arshavsky

_____
Debby Silver

_____
Beth Sullivan

An abstract of a dissertation submitted in partial
fulfillment of the requirements for the degree
of Doctor of Philosophy in the Department of
Pharmacology and Cancer Biology in the Graduate School
of Duke University

2022

Abstract

Projecting neurons of the central nervous system extend their axons through considerable distances from the cell soma. This extreme architecture requires local regulation driven by proteins whose functions are essential for axonal maintenance and survival. Pathways involved in axon survival represent an important question in neurodegenerative conditions like glaucoma. The loss of visual acuity in glaucoma is caused by the degeneration of retinal ganglion cells (RGCs), that transmit visual signals from the retina to the brain. The principal site of RGC axonal insult occurs where the axons exit the eye, weaving through the honeycomb structure of the glial lamina (GL), at the optic nerve head (ONH). While much is understood about the ONH, the specific molecular pathways involved in local regulation of this crucial area is not fully understood. Furthermore, it is not known how these pathways may be altered in glaucoma, which hinders potential therapeutic intervention. Here, we utilize wild-type and glaucomatous mice to decipher the specific proteomic signature of the GL. By Isolating healthy and glaucomatous GL and RL samples, we performed mass spectrometry proteomics analysis to find proteins specifically enriched in the murine GL. Results from wild-type mice showed enrichment of translation proteins in the GL. At the time this thesis is written, proteomics results on glaucomatous mice are not yet available.

Dedication

To those who were not permitted.

Contents

List of Tables

List of Figures

1. Introduction

1.1 Rationale

Projecting neurons of the central nervous system extend their axons through considerable distances from the cell soma. This extreme architecture requires local regulation of many key neuronal processes. These mechanisms are driven by proteins whose functions in the axon are essential for axonal maintenance and survival. Pathways involved in axon survival represent an important question in neurodegenerative conditions like glaucoma [1, 2]. The loss of visual acuity in glaucoma is caused by the degeneration of retinal ganglion cells (RGCs), that transmit visual signals from the retina to the brain. The principal site of RGC axonal insult is located where the axons exit the eye, weaving through the honeycomb structure of the glial lamina (GL in mouse; lamina cribrosa, LC, in human), at the optic nerve head (ONH) [3-9], while the rest of the optic nerve, referred to as the retro-lamina (RL), is affected later in the course of disease. If much is understood about the ONH's anatomy, vasculature supply, and cell types, the specific molecular pathways involved in local regulation of the ONH axons is not fully understood. Furthermore, it is not known how these pathways may be altered in the ONH in glaucoma, which hinders potential therapeutic intervention. Studies assessing changes in the glaucomatous proteome have been done in acute glaucoma models in the retina [10-12], but these studies did not assess chronic models of glaucoma or the ONH specifically, the principle site of axonal damage in glaucoma. To address this, we used wild-type mice and the DBA/2J (D2) model of

glaucoma to assess the global proteomics of the GL and RL. This global approach allows us to capture proteins from all cell types in the region, like astrocytes, which are also involved in axonal regulation [13, 14]. By Isolating healthy and glaucomatous GL and RL samples, we performed mass spectrometry-based proteomics analysis to find proteins specifically enriched in the murine GL. These proteins may play a specialized role in ONH biology with potential implications in axonal maintenance and function. Moreover, proteins altered in glaucoma may point to new avenues for therapeutic intervention.

1.2 The Optic Nerve Head

1.2.1 RGC Axons

The ONH is a specially engineered structure at the back of the eye which allow exit of bundled RGC axons while maintaining intraocular pressure. RGCs are neurons located in the innermost layer of the retina that represent <1% of all retinal cells [15-17]. RGC's main task is to transmit visual information from the eye to the brain. RGC axons collect at the back of the eye and exit, forming the optic nerve [18, 19]. Leaving the eye, RGC axons are squeezed and organized into bundles by astrocytes of the GL. RGC axons project to visual processing regions of the brain including the superior colliculus and lateral geniculate nucleus.

1.3.1 Other components of the ONH

The optic nerve sits in the optic nerve canal, which is the opening of three layers of tissue around the eye. In addition to RGC axons, the ONH includes other cell types and structures. Notable cell types include glial cells like astrocytes and microglia, which

will be covered in the next section. Notably, oligodendrocytes are absent, corresponding to the lack of myelination in the ONH. The ONH also contains a network of artery branches to supply blood to the ONH, and arteries that supply blood to the eye.

1.3.1.1 Vasculature

Blood vessels are present in the ONH, where they enter then eye. Blood vessels supplied from the ophthalmic artery provide nutrients to the eye. The ophthalmic artery is a branch of the internal carotid artery and subsequently branches into the central retinal artery (CRA), posterior ciliary artery (PCA), and collateral branches (Figure #). Most of the blood supply to the eye is from the ophthalmic artery via the CRA and branches of the short PCA [16]. Hayreh (2008) divides the intraorbital optic nerve into anterior and posterior segments based on where the CRA migrates from the peripheral surface to the center of the optic nerve (Figure 1). Anterior and posterior segments correspond the the GL and RL respectively. During development, an invagination of mesenchymal cells, termed the optic fissure, forms the hyaloid artery, which later gives rise to the CRA and determines where the CRA enters into the optic nerve [23, 24]. The anterior optic nerve is nourished by the PCA [16, 31, 32]. The vessels nourishing the prelaminar and laminar regions are either direct branches of the PCA or originate from

the arterial circle of Zinn-Haller (Figure 1) [16].

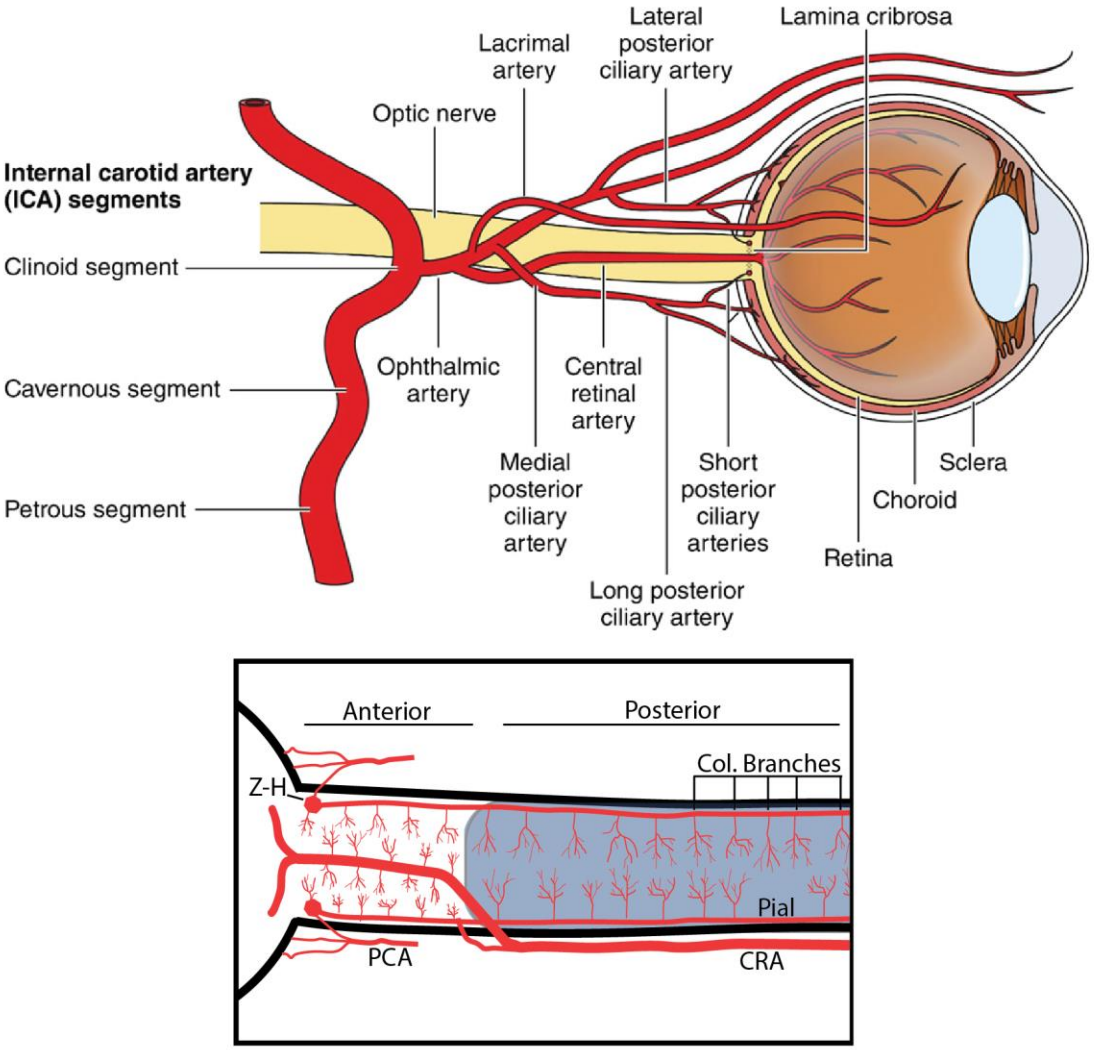

Figure 1: The vasculature of the human optic nerve. (Top) Arteries derived from the internal carotid artery that supply the optic nerve and ONH in human. Image from [20]. (Bottom) The anterior (GL) and posterior (RL) optic nerve are divided by where the CRA traverses to the core of the optic nerve from the periphery. Blue represents the myelinated region of the ON. Col. Branches., collateral branches. CRA, central retinal artery. ICA, internal carotid artery. PCA, posterior ciliary artery. Pial, pial artery. Z-H, Zinn-Haller.

1.3 Non-Neuronal Cellular diversity

Glial cells are non-neuronal cells of the central and peripheral nervous system that provide support to neurons. Astrocytes and microglia are the two glial cell types present in the murine ONH (lamina cribrocytes cells are also present in human ONH) [6, 21-25].

1.3.1 Astrocytes

Astrocytes are the most abundant glial cell type in ONH and are more enriched in the ONH than in the rest of the optic nerve [6, 22, 23]. They serve essential roles in axon structural support, injury response, and mitochondrial degradation. Astrocytes form the honeycomb pattern of the GL, which support RGC axons as they exit the eye. These astrocytes have 6-8 primary processes transversely oriented, running perpendicular to RGC axons creating the honeycomb-like structure [14, 26-29]. Astrocytes in the RL are morphologically distinct from GL astrocytes, with greater heterogeneity in their shape and orientation [30]. Astrocytes are generally quiescent, but become activated in response to stress and inflammation, such as in glaucoma [31, 32].

Astrocytes, along with microglia (discussed later) are known to play a key role in inflammation in the CNS, however little information is available about the optic nerve [33-38]. In the ON, astrocytes help maintain the blood-brain- and blood-retina-barriers (BBB and BRB), by surrounding the endothelial cells of blood vessels, thus creating an immune privileged environment protected from the invasion of peripheral immune cells [37, 39, 40]. When activated by microglia, CNS astrocytes can either become neuroprotective or neurotoxic. Two kinds of activated astrocytes have been identified, named A1 and A2 to match the M1 and M2 nomenclature used for macrophages [36, 41]. In the CNS, A1 activated astrocytes were shown to upregulate a number of genes known to be harmful to synapses (note that synapses are not present in the ONH) and A2 activated astrocytes promoted neuronal survival and growth [42, 43]. Furthermore, it has been shown that A1 astrocytes are generated after optic nerve crush, a

surgical technique used to model an optic nerve injury, and that astrocytes represent the vast majority of proliferating cells in the ONH in a model of glaucoma [22, 36]. It is clear that astrocytes are important in the inflammatory response in the CNS, but limited information is available of what occurs in the optic nerve and ONH. Since much astrocyte research occurs in synapse-dense grey matter of the CNS, it is difficult to extrapolate what occurs in the synapse-deficient fibrous white matter of the optic nerve [33].

GL astrocytes are involved in mitochondrial maintenance for RGC axons. In landmark work from Davis et al., ONH astrocytes were found to degrade axonal mitochondria by phagocytosing axonal evulsions and breaking them down in their lysosomes in a process called "transmitophagy" [13, 44]. While it is unclear why transmitophagy occurs, there are some hypotheses. One possibility is focal axon damage somehow stimulates this process. Another hypothesis suggests that is it too energy intensive for damaged mitochondria to be transported back to the soma, where degradation generally occurs, thus, making it easier for astrocytes to perform this quality control process in RGCs. It is still unknown if non-resident mitochondria are actively transported to the ONH for degradation or if only local ONH mitochondria undergo degradation here [13]. Glaucomatous conditions could result from changes in astrocytic function in the GL including, potentially, transmitophagy. Therefore, it is important to consider their known roles in the ONH, axonal maintenance, and inflammatory response.

1.3.2 Microglia

Microglia are the resident defense cells of the CNS. In the retina and ONH, they function as resident macrophages [45, 46]. Microglia are stellate, or star-shaped, cells with thin ramified processes (Figure 2). They are found throughout the ONH in the walls of large blood vessels and

surrounding capillaries in the glial columns [23]. This glial subtype has a normal or quiescent state and enters an activated state in response to neuronal injury [47-49]. In their normal state, CNS microglia remove cellular debris and surveil the tissue microenvironment to respond to neuronal injury [50-55]. After ONH injury like in glaucoma, the density of microglia in the ONH increases via increased proliferation and migration of activated microglia. [22, 32, 56-58].

The activated state is thought to be protective in early or acute disease, but long-term or hyper-activation can lead to inflammation and degeneration of RGCs [32, 59-61]. In activated microglia, inflammatory cytokines like TNF-α are upregulated [62, 63] and TNF-α has been shown to be abundant in glaucomatous and crushed ON, but not in normal optic nerve [32, 62]. After an optic nerve crush, TNF-α expression in microglia is reported to protect RGCs and helps with tissue maintenance and regeneration [62, 64]. However, in a mouse model of traumatic brain injury, TNF-α is suggested to be associated with RGC loss [65]. Other experiments in animal models of glaucoma show inhibiting TNF-α prevents RGC apoptosis and inflammation and inhibiting microglial activation also reverses RGC cell death [66-71]. Long-term upregulation of inflammatory marker genes and an increase in the release of ROS and NO is also associated with RGC loss [63, 72].

Microglia also activate astrocytes, which can be either neuroprotective or neurotoxic (discussed previously). Depletion of microglia in optic nerve injury showed that RGC degeneration was unaffected, however, astrocyte repopulation at the site of optic nerve injury was

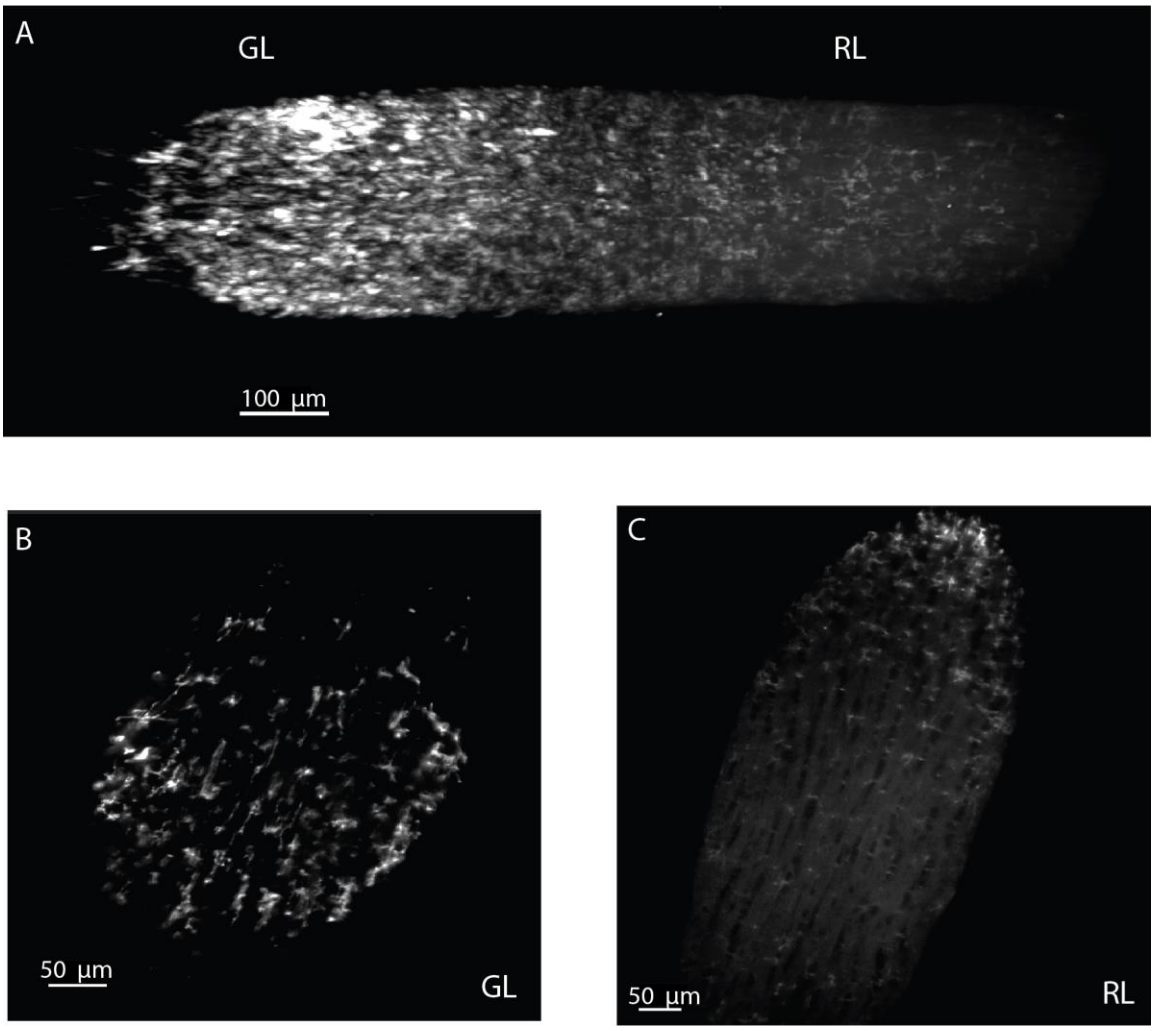

Figure 2: Light sheet fluorescent microscopy images show that P2Y12-stained microglia have increased abundance in the GL. (A) 3D reconstruction of the longitudinal view of stained microglia in the optic nerve. (B) Cross section of the GL shows microglia. (C) Cross section of the RL shows few microglia. Image credit: Samantha Wilkinson and Daniel Saban.

significantly delayed upon microglia depletion, indicating that microglia may be involved in optic nerve regeneration in acute injury conditions [73]. Recent studies have demonstrated mitochondrial fragmentation in microglia can regulate astrocyte activation [74].

In summary, microglia and astrocytes have important functions in the ONH and to the diverse cellular environment of the ONH. Astrocytes are the most abundant glia cell type in the ONH, providing structural support to RGC axons and becoming activated in response to injury. Microglia are involved in removing cellular debris and surveilling the tissue microenvironment. Both glial cell types become activated a part of the injury response, which is relevant in the context of the neurodegenerative disease glaucoma.

1.4 Glaucoma

Glaucoma is a group of diseases that damage the optic nerve, leading to visual impairment. Primary open angle glaucoma (POAG), the most common type of glaucoma, is estimated to affect 68.56 million people worldwide, or 2.4% of the population [75-77]. Glaucoma is the leading cause of untreatable blindness and is characterized by the death of RGCs and their axons which leads to progressive visual field loss and eventual blindness [78]. High intraocular pressure (IOP) is a widely recognized risk factor for developing POAG and clinical evidence supports that lowering IOP reduces onset and progression of glaucoma [79-81]. However, lowering IOP is not universally helpful in preventing or slowing glaucoma. For example, in a study placing patients with early-stage glaucoma in a IOP-reducing treatment or control group, 45% in the treatment group still had progression of glaucoma compared to 62% in the control group [82]. This study demonstrates that decreasing IOP is not always enough to prevent disease progression. Age is another key risk factor in glaucoma. Age is important because many characteristics of the ONH that change with age are hypothesized to make the eye more susceptible to glaucomatous neurodegeneration

[83]. These involve changes in the density of axon packing [83], metabolism [84], mitochondrial function [85-87], and connective tissue stiffening in the sclera and LC [88-92]. When reducing IOP is insufficient to stop glaucoma onset or progression, other factors like those that change with age could be involved. However, RGC degeneration in normal tension glaucoma is still very much a mystery in the field. Therefore, further research is needed to better understand disease progression unexplained by a high IOP.

1.4.1 Models of glaucoma

There are varied models of experimental glaucoma, each having its own ideal uses and experimental requirements. There are chronic models in which disease pathology develops over time and acute models that more rapidly induce disease-like phenotypes. Classic examples of these two types of models are the chronic genetic model DBA/2J (D2) mouse, and injection of microbeads into the anterior chamber to increase IOP acutely.

D2 mice have been the standard pre-clinical model for glaucoma, most-widely published model, and well-characterized. These mice have mutations in melanosomal proteins, that results in chronic age-related pigmentary glaucoma sharing many similarities with the human condition [93, 94]. The melanosomal protein mutation are the recessive *Tyrp1*^{b} mutant allele and a premature stop codon mutation in the Gpnmb (*Gpnmb*^{R150X}) gene [95]. Non-glaucomatous control of the D2 mice have been generated (D2+) on same genetic background as the D2 mouse but lacking the mutations in *Gpnmb* and *Tyrp1* [96]. In D2 mice, IOP spontaneously increases around 9 months of age, with

important animal to animal variability [6, 96, 97]. Although this variability produces what is seen in human glaucoma, it poses obvious experimental challenges.

Conversely, acute models have lower variability and do not require aging mice. For example, one acute model like microbead injection will reliably increase IOP and trigger RGC loss [98]. However, the RGC loss in this model is only around 20-30% depending on the beads used although with low variability [98]. Another acute model, high-dose intravitreal administration of glutamate, causes rapid loss of RGCs, with signs of apoptosis seen in as little as one hour. Low-dose glutamate (injected every 5 days) can also be used to trigger 42% RGC death within three months [99]. While acute models can be more efficient for testing pharmaceuticals, slow changes like in the D2 mouse model better recapitulate the chronic and slow-moving human glaucoma. Additionally, since in the present study we aim to capture pre-disease state following IOP degeneration and before RGC loss, a longer period between IOP elevation and RGC loss is experimentally favorable.

2. Results

2.1 The Mouse Glial Lamina can be Robustly Isolated from the Optic Nerve

To be able perform proteomics and other biochemical assays on the GL, it was necessary to specifically isolate this small region of the ONH. To achieve this, we first removed the eye and the whole optic nerve from the skull under a dissection scope. At this stage, the GL could clearly be identified by its transparent aspect due to the lack of myelination (Figure 3B). We then dissected out the GL as well as a portion of the RL of similar size (~200µm). The RL was identified thanks to its opacity due to myelination (Figure 3A and B). To assess the specificity of our dissection procedure, we extracted proteins from the GL and RL and ran them on a western blot. As shown in Figure 3C, we showed that the GL was successfully dissected out. We use myeline basic protein (MBP) to confirm the lack of myelin in our GL samples. As expected, MBP signal in both the retinal control lane and the GL lane was absent whereas it was strong in the RL lane. This result suggests our approach allows for a specific dissection of the GL from the myelinated RL

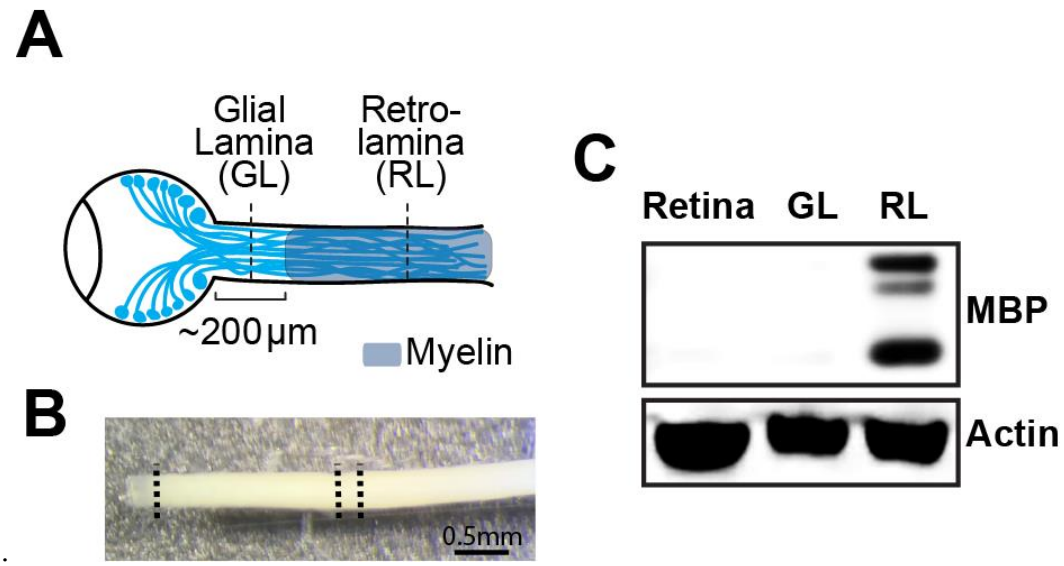

Figure 3: The dissected GL region of the optic nerve lacks MBP, showing specific dissection. (A) A diagram of the eye and optic nerve shows RGCs (blue) and myelin (grey), representing the location of GL and RL regions. (B) Dissection scope image of the optic nerve with the GL (clear) on the far left and RL dissection sample outlined on the right. (C) Western blot showing GL samples can be cleanly separated without MBP.

2.2 GL Proteomics Reveals an Enrichment in Proteins Related to Translation

To uncover molecular regulators of the GL, we next wanted to qualitatively compare protein content of the GL and RL optic nerve. We hypothesized that the high specific structure of the GL was coupled with GL specific functions that could be revealed by deciphering the proteomic signature of the GL. To test this hypothesis, we performed mass spectriomtry of GL protein extract from wild-type mice. Three independent isolations and proteomic runs were performed using 7-8 GL and RL optic nerve samples isolated from 4-5 mice per replicate. In each run, we calculated the abundance ratio of GL over RL for every protein detected to obtain a fold-change. A cut

off was set at 2.0-fold-change as proteins considered enriched in the GL. This list of enriched proteins was imported for gene ontology (GO) analysis. Surprisingly, this analysis revealed that ribosomal and translational proteins in the GL samples were consistently enriched across replicates (Figure 4). GO terms such as mRNA processing

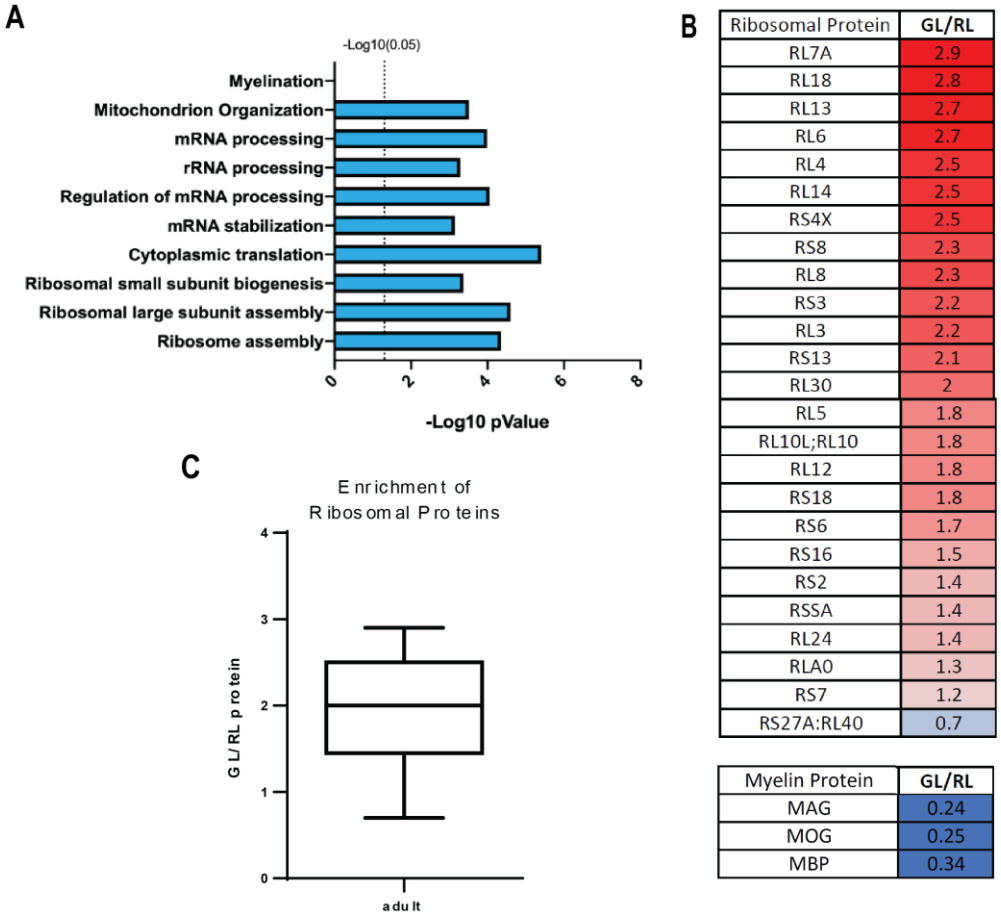

Figure 4: Enrichment of protein related to translation is shown in wild-type proteomics. (A) GO analysis of GL enriched proteins show a significant increase in translation and mitochondrial proteins. The term myelination did not appear in GL GO analysis, but does in RL. (B) Ribosomal large and small subunit proteins are enriched in the GL. Detected myelin related protein enrichment is shown at the top. (C) Ribosomal proteins are enriched on average 2.0-fold in the adult GL (n=25).

and stabilization, cytoplasmic translation, ribosomal biogenesis and assembly were significantly overrepresented (Figure 4A). We also detected enrichment of many mitochondrial proteins, which was anticipated based on the increased number of mitochondrial in GL axons [100].

2.3 DBA/2J Model Validation and Proteomic Sample Selection

Next, we asked whether the proteomic signatures detected in wild-type mice GL, namely increased translation-related proteins, would be affected in the context of a neurodegenerative stress. Studies on proteome changes have been done in acute glaucoma models in the retina [10-12], but not specifically in the GL nor in a chronic model. To answer this question, we used the DBA/2J (D2) glaucoma model and its control D2-*Gpnmb*+ (D2+). We first conducted thorough long-term measurements of IOP and analyzed RGC loss to validate this model in our hands and minimize variability in analysis.

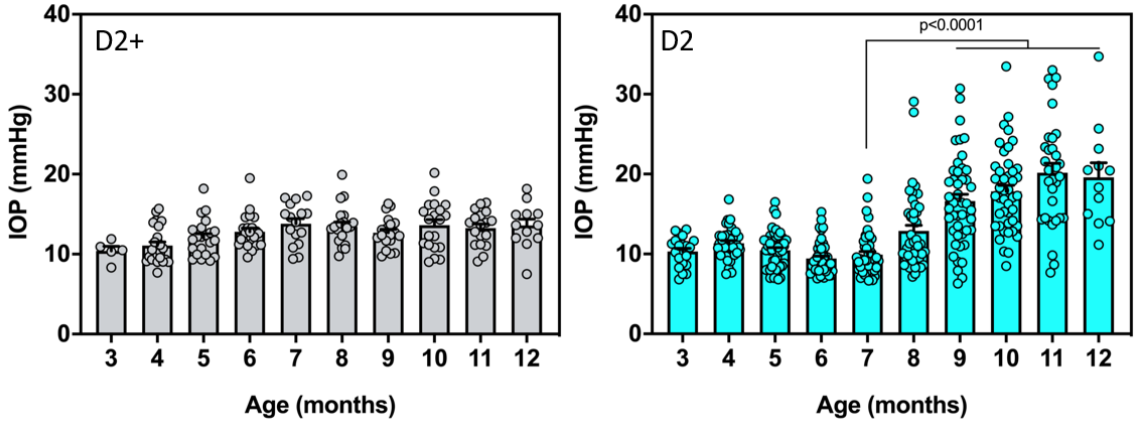

Figure 5: Intraocular pressure of D2+ and D2 mice from three to twelve months. Statistics are Kruskal-Wallis multiple comparison with Dunn's correction. D2 n=4-19. D2+ n= 12-43.

The IOP of each mouse was measured weekly from three to twelve months to determine how IOP changes over time. As expected, D2+ control mice exhibited no change in their IOP over the time measured (Figure 5, left). However, D2 mice showed a statistically significant increase in IOP nine to twelve months compared to seven months of age which represent the baseline IOP (Figure 5, right). This result is in accordance with literature [6, 96, 97]. Therefore, we confirmed that (i) we could robustly monitor IOP in these mice and (ii) this model is valid as a glaucoma model. In addition to model validation, data collection on the IOP and RGC loss in each mouse allowed for specific selection of pre-disease state mice for inclusion in our proteomic studies.

As reported by others, the IOP of D2 mice shows vast variation between animals, where some animal never develops increased IOP (Figure 5, right) [6, 96, 97]. To make sure that each D2 mouse we selected for proteomics analysis has indeed a high IOP, we

developed a two-step selection strategy. The first step is to select mice that exhibit a high IOP, the greatest glaucoma risk factor. Our regular and thorough recording of IOP of each individual mouse, allowed us to specifically select mice that exhibit high IOP, thus eliminating the substantial variability in IOP in pre-disease state. Indeed, it is well established that high IOP precedes axonal degeneration in nine-to-ten month mice [97]. Similar strategies of selecting certain D2 mice based on their physiological data have been noted in other studies [101].

The second step of the two-step selection process is to select for mice that do not already exhibit degeneration of RGCs. Since our goal is to study a pre-disease state to monitor the effector of glaucomatous stress on the proteins present specifically in the GL and RL, it is key that we select for mice in a stage that precedes the onset of neurodegeneration. Therefore, we performed RGC survival analysis on the retina of the selected high-IOP mice. The abundance of RGCs was determined by staining RGC some in the retina with the RGC marker RBPMS and counting the positive soma in FIJI. Example images from D2+ and D2 mice are shown in Figure 6A. As expected D2+ control mice do not show a decrease in the number of RGCs at any age. However, some D2 mice show a decrease in RGCs already at 9-10 months and 12 months (Figure 6B). We noticed by analyzing this data there is a bi-modal distribution in both the D2 9-10 months and 12 month groups, where some mice lose RGCs and some do not (Figure 6B). Since all the mice in this cohort have been selected for a high IOP, a variability in IOP is

unlikely to account for this difference in RGC degeneration. Leaning on the strength of our comprehensive recording of each individual mouse analyzed, we looked at each data point and isolated other potential factors that could account for this difference and found that the sex of mice accounted for this bi-modal distribution.

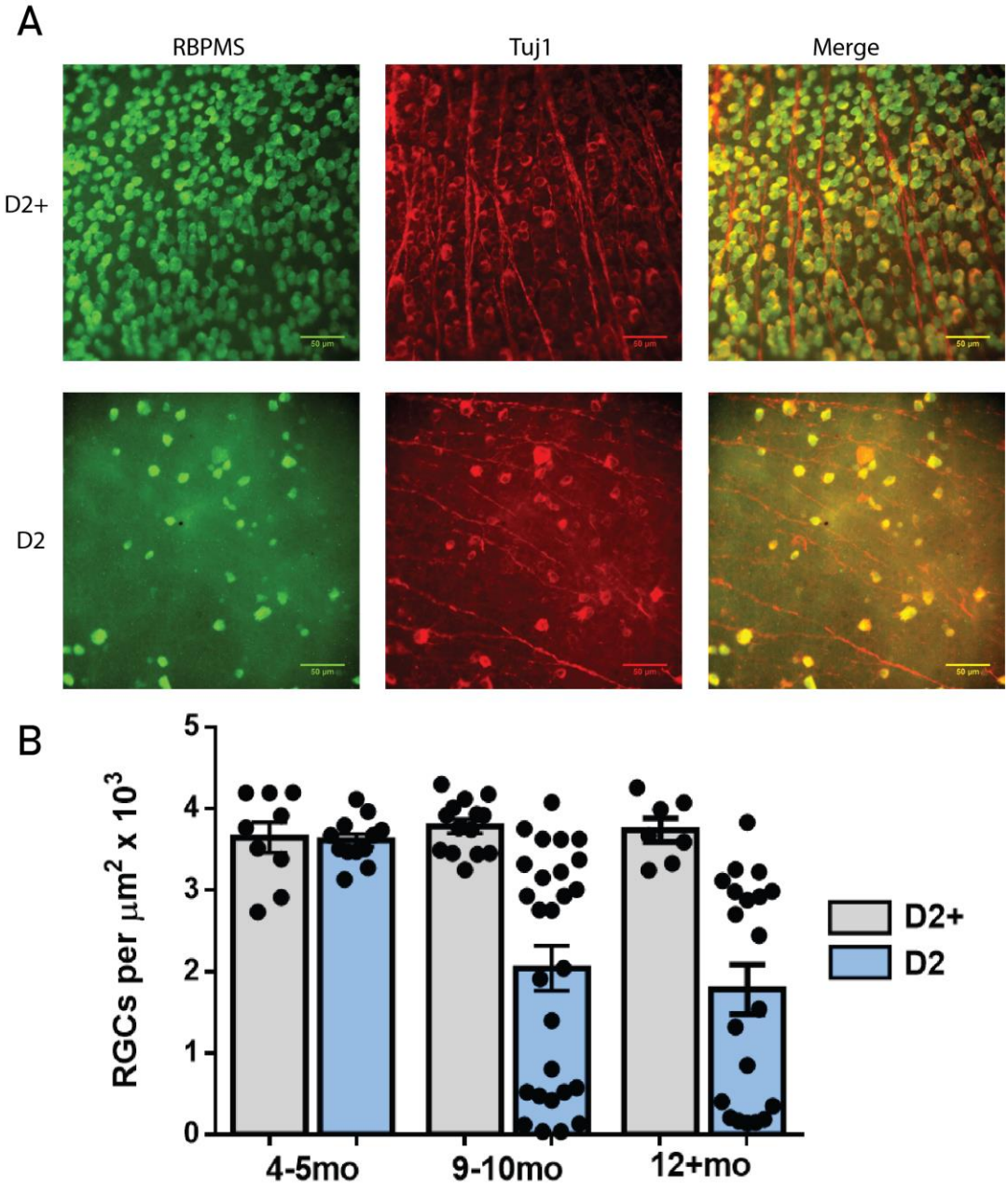

Figure 6: RGC images and counts in healthy (D2+) and glaucomatous (D2) retinas at 4-5 months, 9-10 months, and 12+ months. (A) Images from 9-10 month old D2+ and D2 mice stained with RBPMS and Tuj1. (B) RGC counts from D2+ and D2 mice. 4-5 months: D2+ n=9, D2 n=12. 9-10 months: D2+ n=14, D2 n=27. 12+ months: D2+ n=7, D2 n=19.

Indeed, we separated mice by sex to determine if this accounted for the bi-modal distribution. Surprisingly, this distribution clearly separates based on sex, with female mice losing RGCs and males remaining normal at 9-10 months (Figure 7A, B). Interestingly, there is a statistically significant decrease in RGCs in the 9-10 and 12 month old female mice (Figure 7C). Since we are selecting for a pre-disease state with RGCs still present, female mice have been excluded from the proteomic analysis. To further assess potential sex differences between mice, we also asked if the variability in IOP is impacted by sex.

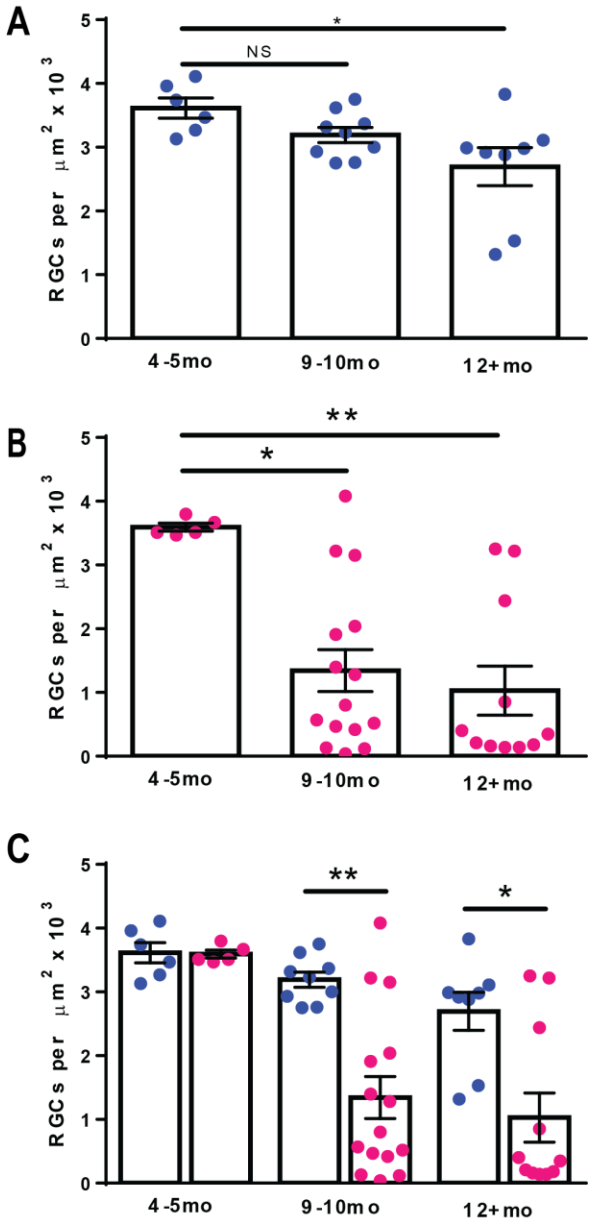

Figure 7: RGC counts decrease in female mice. All mice were dissected after IOP increase. (A) RGC counts in male mice. (B) RGC counts in female mice. (C) Comparison of male and female RGC counts. 4-5 months: male n=6, female n=5. 9-10 months: male n=9, n=15. 12+ months: male n=8, female n=11. A&B: Kruskal-Wallis non-parametric test. C: Unpaired t-test with age groups. * p<0.05, ** p<0.01, ***p<0.001.

To determine if the RGC loss in female mice was related to higher IOP, we compared IOP by sex. An earlier or greater increase in IOP could explain the greater loss of RGCs in 9-10-month and 12-month-old D2 female mice. When IOP is compared by sex, we didn't observe a difference in IOP at any age group between male and female mice (Figure 8). This suggests that IOP is not the reason that female D2 mice have greater loss of RGCs.

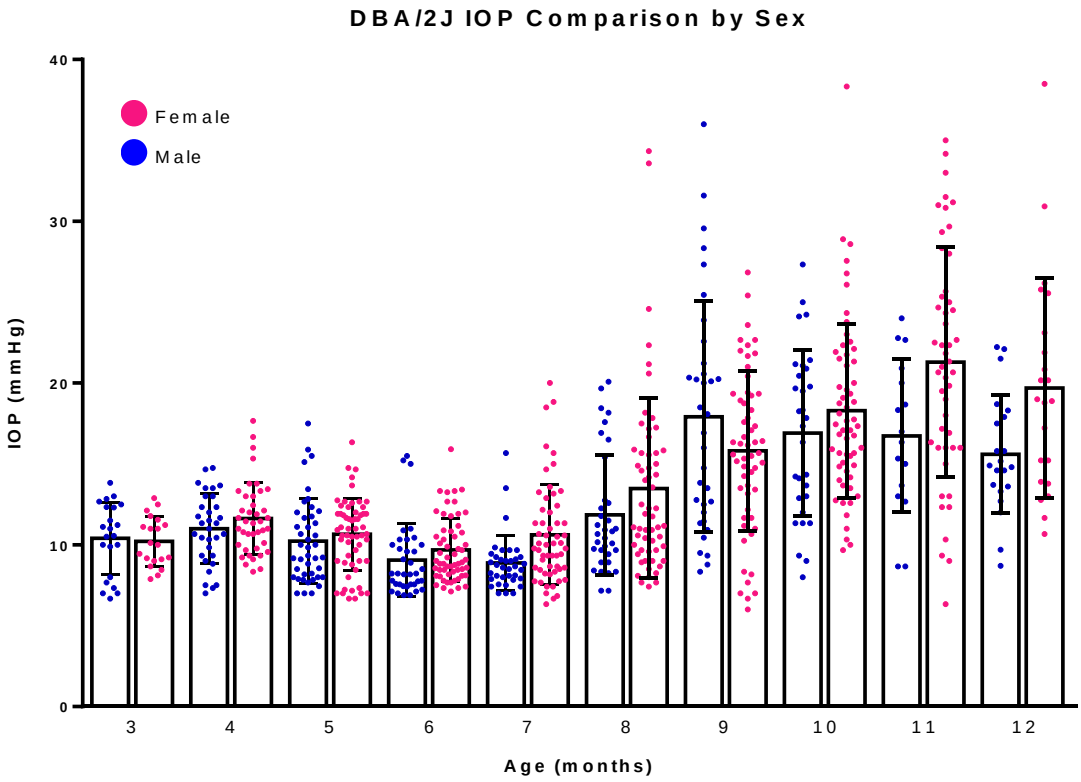

Figure 8: IOP of D2 mice separated by sex. There are no differences in IOP between male and female mice. n=16-58

2.4 Optic Nerve Head Proteomics Sample Size Selection

The time- and labor-intensive process of selecting pre-disease state DBA/2J glaucoma mice makes the tissue samples precious and hard to replace. Initially working with both sexes, half of our aged group already showed RGC degeneration, excluding them from the pre-disease state we desired. Also, some mice aged out of the timepoint without showing high IOP, meaning they also failed our two-step validation process. Each experimental mouse resulted in substantial time aging mice and labor of collecting weekly data. Data collection far exceeds just the mice included in our proteomics, since female mice were excluded due to RGC loss and not all mice exhibited increased IOP.

Due to the precious nature of the samples, we performed an experiment to determine the minimum number of optic nerve samples (GL and RL) that needed to be included in the proteomic analysis. For this experiment, we performed mass spectrometry analysis using two, four, six, and eight GL and RL samples. The goal of this experiment was to determine the amount of tissue needed for reliable protein detection by mass spectrometry. As a proxy for detection efficiency, we used ribosomal and mitochondrial proteins categories of proteins we knew from previous experiments were enriched in the GL. The number of enriched proteins detected increased with the amount input tissue, with the exception of the one with four tissue samples showing the smallest number of enriched proteins (Figure 9A). This could be due to variation in the sample preparation or in the proteomics itself. Mitochondria proteins were identified

using a list of mitochondrial proteins, MitoCarta3.0. Ribosomal proteins

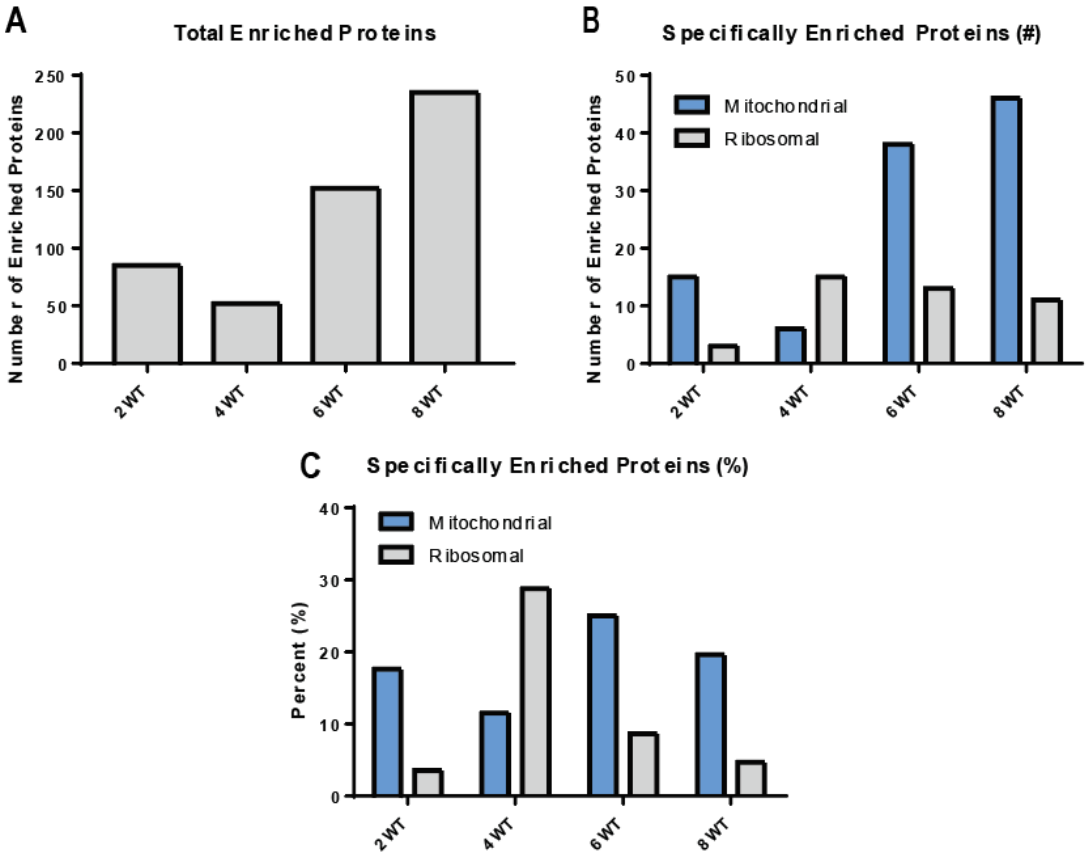

Figure 9: Assessment of two, four, six, and eight optic nerve proteomics. (A) Total number of 2.0-fold enriched proteins detected in each sample. (B) The total number of ribosomal and mitochondrial proteins that are enriched. (C) The percent of total detected enriched proteins that constitute either ribosomal or mitochondrial proteins.

were identified as all large and small ribosomal subunit proteins. While four tissue samples had the lowest number of enriched proteins, nearly 30% of them were ribosomal and over 10% were mitochondrial (Figure 9B, C). Four tissue samples appears to be an anomaly, as two, six, and eight showed 3.5-8.6% of enriched proteins as mitochondrial. In the case of two, six, and eight tissue samples, the number of

mitochondrial proteins is three- to five-fold greater than ribosomal proteins, showing a similar trend between groups. There does not appear to be improved detection of ribosomal and mitochondrial proteins between six and eight tissue samples, therefore six tissue samples was the number selected to use in the glaucoma proteomics experiment.

2.5 Utilizing the Two-step Selection of Samples for Proteomics

The mass spectrometry analysis on glaucoma samples will be run in duplicate and at the time this thesis is written we are awaiting the collection of samples to be completed. By taking advantage of our two-step selection process, groups for proteomic analysis will possess less variability compared to the whole cohort of mice from which we collected data.

3. Discussion

3.1 Proteomics in Wild-type ONH and Glaucoma Expectations

One of the group of proteins that were enriched in the GL of the ONH in wild-type mice was ribosomal proteins and other proteins related to translation. Although our global approach captures proteins from all cell types, it is tempting to speculate that this proteomics signature is coming from RGC axons. First reported in the 1960s, the idea of local protein synthesis in axons faced skepticism due to impure axonal samples and limitations in ultrastructural evidence for the presence of ribosomes in axons. Only in recent years have technical advances led to the broad acceptance of local axonal protein synthesis [102-105].

Local protein synthesis is a highly conserved mechanism, and this is particularly important in axons, which require proteins for specialized functions far away from the nucleus [106-108]. If these proteins had to travel from the neuronal soma, the time lag would be too long for most axonal function. Interestingly, hotspots of axonal translation are correlated with the presence of mitochondria [105, 109], which are highly enriched in the ONH axons [6, 13, 22, 100, 110-117]. It was long assumed that mitochondria were enriched at the ONH due to the absence of myelination and higher energy expectations of these axons. However, it was recently reported by our group that mitochondrial accumulation in the ONH precedes myelination, suggesting that energy demands of unmyelinated axons are not causative of the accumulation [100]. This result raises the

question of the reason of this local enrichment of mitochondria. Based on the results presented here, one can speculate that it could be related to increased local translation. Mitochondria could be present to provide energy to translation, which is an energy-consuming process [118, 119]. It has been reported that mRNA translation in axons occurs on Rab7a endosomes, which often pause on mitochondria [120]. Rab7a was detected in our wild-type proteomics, but it did not show any enrichment in the GL. It is also known that local translation of mitochondrial proteins is essential for mitochondrial function in axons [121-123]. Further work is needed to answer key questions, such as what cell type(s) is over expressing this class of proteins and what these ribosomes enriched in the ONH are translating.

In assessing proteomics of glaucomatous GL, we hypothesize that a neurodegenerative stress could alter the translational signature seen in wild-type mice. At the time this thesis is written, proteomics results on glaucomatous mice are not yet available. However, one can anticipate a possible outcome. As mentioned earlier, translation in RGC axons has been found to occur on late endosomes paused on mitochondria and they are known to translate mitochondrial proteins that are essential for axonal maintenance [120]. If there is a change in the translational signature, but no change in the mitochondrial protein signature, one interpretation is that translational changes precede mitochondrial dysfunction seen in glaucoma. Such result would open new research avenues in glaucoma as this concept is complete unexplored. Broadly,

changes in the GL proteomic signature in glaucoma could also point to new potential therapeutic targets.

3.2 Sex Variation

Our analysis of RGC survival in D2 glaucomatous mice showed significant differences between male and female mice. Female mice exhibited significantly fewer RGCs than male mice at 9-10 and 12+ months of age (Figure 5c). Moreover, female mice showed significant RGC loss starting at 9-10 months, while males did not show significantly RGC loss until 12+ months of age (Figure 5a, b). In humans, some sex-specific differences have been reported in glaucoma susceptibility, but not all studies support this [80, 124-127]. Additionally, some groups report sex variation in D2 mice while others do not. One group assessing the prevention of visual impairment in D2 mice using a glaucoma drug found no sex difference in response. However, this group did not assess IOP or RGC loss [128]. Another study characterizing important disease features in DBA/2J mice noted that female mice tended to have increased IOP earlier than males, with significant differences at 6-7 months, but similar at 8-9 months [97]. However, we found no differences in IOP based on mouse sex in our own IOP data (Figure 6). Libby *et. al* also assessed optic nerve damage in these mice using paraphenylenediamine (PPD), which stain myeline sheaths and darkly stains sick and dying axons, providing a qualitative assessment of optic nerve health. Minor sex differences in optic nerve damaged were noted in this study, but they did not observe

the stark bi-modal pattern seen in our RGC count data [97]. Of significance, our data provides a quantitative assessment of RGC number as opposed to a qualitative assessment of optic nerve axon damage. In comparison to Libby *et. al*, another study corroborates the higher IOP in females at 6-month timepoint, but sees this trend remain and become more pronounced rather than normalize between groups. This study does not comment on if these different in IOP impact RGCs or nerve damage [101]. Therefore, our finding that RGC loss occurs months earlier in female D2 mice comparing to males has not been confirmed by other studies that only noted small differences when comparing optic nerve axon health between sexes. This could be due to the fact they studied mice not previously selected for by a high IOP. Another possibility could be the role played by environmental factors present in our animal house. Indeed, other D2 mice phenotypes have been shown to be dependent on housing conditions (Dr. Simon John, personal communication).

3.3 Future Directions

At the time this thesis is written, all GL and RL samples for both D2 and D2+ have been collected and are being prepared for duplicate proteomics runs. The next steps will be to analyze these results to determine the proteome changes in the GL with age and in glaucoma. Additionally, we will use EM to verify that degeneration is not occurring in ONH in the 9-10 month D2 mice selected as pre-disease state. This would

verify that mice without RGC loss in the retina also do not have signs of axonal degeneration in the ONH, the initial site of insult.

Based on our proteomic results from wild-type mice highlighting the enrichment of proteins involved in translation, we plan to assess if ribosomes are enriched in GL when compared with the RL region. This would add support to the idea of local axonal protein synthesis in the GL. To determine if ribosomes are present in RGC axons, we will utilize the RiboTag mouse, which expresses a HA tagged Rpl22 ribosomal protein. By crossing the RiboTag mouse with the Vglut2Cre driver mouse we will ensure the tagged Rpl22 will be expressed in RGCs. The presence of ribosomes will then be assessed using western blot and immunofluorescence. Furthermore, using the same mouse, we will next probe what mRNA GL ribosomes are translating using ribosomal pull down and translatomics. This will provide greater insight into the function of ribosomes in the GL.

4. Methods

4.1 Animal Models

Experiments using mice were approved by the Duke University Institutional Animal Care and Use Committee (protocols A194-20-10). The mice were housed under a 12 h light-dark cycle with ad lib access to food and water. Heat and humidity were maintained within the parameters specified in the National Institute of Health Guide for the Care and Use of Laboratory Animals. Experimental procedures were also consistent with this Guide. Wild-type C57BL/6J mice (The Jackson Laboratory stock 000664) were used for the proteomics study on healthy GL and RL areas. DBA/2J glaucomatous mice (D2, The Jackson Laboratory stock 000671) and D2-*Gpnmb*+ strain (D2+, The Jackson Laboratory stock 007048) was used as a genetically matched non-glaucomatous control.

4.2 Western Blot

Proteins were extracted using lysate buffer. Samples were boiled for ten minutes, then chilled on ice prior to loading. The Invitrogen Mini Cell gel system was used with Invitrogen NuPAGE 4-12% Bis-Tris pre-poured gels (Catalogue NP0323BOX). The entire sample was loaded and run at 50V through stacking, approximately 20 minutes, and at 100V to finish separation, approximate 60-120 minutes depending on desired separation. Gel was transferred onto Biorad Immun-Blot PVDF membrane (catalogue 1620264) activated with methanol using the Invitrogen Mini Cell transfer system. Transfer was run at 30V for one hour at room temperature. Following transfer, membrane was blotted

with Li-Cor Intercept Blocking Buffer (Catalogue 927-700001) for 45 minutes on a shaker at room temperature. After three five-minute washes in 0.0125% PBST, primary antibody (Table 1) diluted in 50% blocking buffer and 50% 0.0125% PBST was added. Blot was incubated on a shaker at 4°C overnight. After three five-minute washes in 0.0125% PBST, secondary LiCore antibodies (Table 1) diluted at 1:15,000 in 50% blocking buffer and 50% 0.0125% PBST was added. After one hour shaking at room temperature the blot was washed again three times during five-minute in 0.0125% PBST. The blot was then imaged using LiCore Odyssey CLx. Image processing was performed in Image Lab.

Table 1: Antibodies

Primary Antibodies				
Antibody	**Raised in**	**Dilution**	**Observed MW**	**Catalogue No.**
β-ACTIN	mouse	1:2,000	43 kDa	LiCore 926-42212
MBP	rabbit	1:1000	14-20 kDa	Abcam 218011
RBPMS	rabbit	1:1000	22 kDa	Novus NBP2-20112
Tuj1	mouse	1:1000	50 kDa	R&D Systems MAB1195
Secondary Antibodies				
AlexaFlour488	rabbit	1:1000	-	Invitrogen A-11008
AlexaFlour594	mouse	1:1000	-	Invitrogen A-11005
LiCore, 800 CW Donkey anti-Rabbit	rabbit	1:15,000	_	LiCore 926-32213
LiCore 680LT Goat anti-mouse	mouse	1:15,000	_	LiCore 925-68020

4.3 Intraocular Pressure Measurement

Intraocular pressure (IOP) of D2 and D2+ mice was measured weekly, or every other week, using the rebound tonometer from iCare. Mice were placed under light sedation using isoflourine at 4%, 2L/min. Three measurements were taken for the right and left eye. Each week measurements were taken, an average IOP value of each eye (right and left) was calculated from the three measurements, as well as an average for both eyes from the six measurements to determine the IOP trend for each mouse. These data from weekly IOP measurements were then used to calculate the monthly IOP average. All measurements for each individual mouse were recorded to determine their baseline IOP and any changes that occurred with age.

4.4 Tissue collection

Mice were perfused intracardially with PBS for five minutes to remove blood. Cervical decapitation was performed, and the eye and GL and RL optic nerve samples were collected. The optic nerve samples (GL and RL) were then flash frozen in liquid nitrogen and stored at -80°C. The eye was punctured through the pupil (avoiding damage to the retina) and fixed in 4% PFA for one day, then kept in PBS at 4°C. Wild-type mice were dissected at 8 weeks of age. D2 and D2+ mice were dissected at between 4 and 5 months and between 9 and 10 months old. 9–10-month-old D2 mice were collected once an IOP higher than that mouse's baseline was consistently detected.

4.5 RGC Counts

For each mouse from which we obtained GL and RL samples, the retina was dissected from the fixed eye and cleaned of debris. The retina was placed in a 1.5 mL Eppendorf tube with blocking solution (3% donkey serum + 0.3% Triton X-100 in PBS) and rocked for one hour at room temperature. Primary antibody for RBPMS and Tuj1 were diluted in blocking solution (see Table 1 for antibody details), and 200µL was added to each tube. Retinas stained in primary on a rocker at 4°C overnight. The next day, primary antibody was removed, and retinas were washed on a rocker at room temperature with 1X PBS, changing the PBS three times during the wash. Secondary antibody was diluted in 0.3% Triton X-100 and 200µL was added to each tube. Secondary antibody incubation occurred on a rocker at room temperature for 1-2 hours. Following secondary antibody incubation, retinas were washed on a rocker at room temperature with 1X PBS, changing the PBS three times during the wash. Retinas were cut into a four-leave clover pattern and place inside up on a MF-Millipore 0.45 µm Blk gridded filter (REF HABG01300) on top of a filter paper. Once the PBS was absorbed by the filter paper, allowing the retina to lay flat on the gridded filter, the gridded filter was transferred to a slide. The retina was flat mounted with Southern Biotech Flouromount-G (Cat No 0100-01) and set with a coverslip. After allowing the Flouromount-G to set overnight, the flat mounted retinas were imaged at 40X using the Nikon Eclipse Ti2 microscope. An image of the inner, middle, and outer regions was taken from each

quadrant of each retina, totaling twelves images per retina. The RBPMS positive RGC soma were counted using FIJI. The average of RGC soma was calculated for the twelve images.

4.6 Mass Spectrometry Proteomics and Analysis

4.6.1 Sample Preparation and LC-MS/MS analysis

For each sample, 6-8 optic nerve samples were used to prepare peptide mixtures for proteomic profiling. Proteins were cleaved with the trypsin/endoproteinase LysC mixture (Promega, V5072) using the paramagnetic beads-based method (Hughes CS et al Mol Syst Biol 2014, 10, 757). Each digest was dissolved in 12 μl of 1/2/97% (by volume) of the trifluoroacetic acid/acetonitrile/water solution, and 3 μl were injected into a 5 μm, 180 μm×20 mm Symmetry C18 trap column (Waters) in 1% acetonitrile in water for 3 min at 5 μl/min. The analytical separation was next performed using an HSS T3 1.8 μm, 75 μm×200 mm column (Waters) over 90 min at a flow rate of 0.3 μl/min at 55°C. The 5-30% mobile phase B gradient was used, where phase A was 0.1% formic acid in water and phase B 0.1% formic acid in acetonitrile. Peptides separated by LC were introduced into the Q Exactive HF Orbitrap mass spectrometer (Thermo Fisher Scientific) using positive electrospray ionization at 2000 V and capillary temperature of 275°C. Data collection was performed in the data-dependent acquisition (DDA) mode with 120,000 resolution (at m/z 200) for MS1 precursor measurements. The MS1 analysis utilized a scan from 375-1500 m/z with a target AGC value of 1.0e6 ions, the RF lens set

at 30%, and a maximum injection time of 50 ms. Advanced peak detection and internal calibration (EIC) were enabled during data acquisition. Peptides were selected for MS/MS using charge state filtering (2-5), monoisotopic peak detection and a dynamic exclusion time of 20 sec with a mass tolerance of 10 ppm. MS/MS was performed using HCD with a collision energy of 30±5% with detection in the ion trap using a rapid scanning rate, AGC target value of 5.0e4 ions, maximum injection time of 150 ms, and ion injection for all available parallelizable time enabled.

4.6.2 Protein Identification and Quantification

For label-free relative protein quantification, raw mass spectral data files (.raw) were imported into Progenesis QI for Proteomics 4.2 software (Nonlinear Dynamics) for duplicate runs alignment of each preparation and peak area calculations. Peptides were identified using Mascot version 2.5.1 (Matrix Science) for searching the UniProt 2019 reviewed mouse database containing 17,008 entrees. Mascot search parameters were: 10 ppm mass tolerance for precursor ions; 0.025 Da for fragment-ion mass tolerance; one missed cleavage by trypsin; fixed modification was carbamidomethylation of cysteine; variable modification was oxidized methionine. Only proteins identified with 2 or more peptides (Mascot scores >15 for a peptide and >50 for a protein corresponding to protein FDR <1% and peptide FDR < 0.5% calculated using reversed decoy database), were included in the protein quantification analysis. To account for variations in experimental conditions and amounts of protein material in individual LC-MS/MS runs, the

integrated peak area for each identified peptide was corrected using the factors calculated by automatic Progenesis algorithm utilizing the total intensities for all peaks in each run. Values representing protein amounts were calculated based on a sum of ion intensities for all identified constituent non-conflicting peptides. Protein abundances were averaged for two duplicate runs for each sample and ratio between samples of interest was calculated.

4.7 Statistics

Statistical analysis was performed using GraphPad Prism software. Specific sample size, statistical test and *p*-values for each experiment are given in the appropriate figure legends. *P*-value less than 0.05 was considered significant. Standard error bars are shown on graphs.

References

1. Kaeslin, M.A., et al., *Changes to the aqueous humor proteome during glaucoma.* PLoS One, 2016. **11**(10): p. e0165314.

2. Mirzaei, M., et al., *Age-related neurodegenerative disease associated pathways identified in retinal and vitreous proteome from human glaucoma eyes.* Scientific reports, 2017. **7**(1): p. 1-16.

3. Quigley, H.A. and E.M. Addicks, *Regional differences in the structure of the lamina cribrosa and their relation to glaucomatous optic nerve damage.* Archives of ophthalmology, 1981. **99**(1): p. 137-143.

4. Anderson, D.R. and A. Hendrickson, *Effect of intraocular pressure on rapid axoplasmic transport in monkey optic nerve.* Investigative ophthalmology & visual science, 1974. **13**(10): p. 771-783.

5. Quigley, H. and D.R. Anderson, *The dynamics and location of axonal transport blockade by acute intraocular pressure elevation in primate optic nerve.* Investigative ophthalmology & visual science, 1976. **15**(8): p. 606-616.

6. Howell, G.R., et al., *Axons of retinal ganglion cells are insulted in the optic nerve early in DBA/2J glaucoma.* The Journal of cell biology, 2007. **179**(7): p. 1523-1537.

7. Jakobs, T.C., et al., *Retinal ganglion cell degeneration is topological but not cell type specific in DBA/2J mice.* The Journal of cell biology, 2005. **171**(2): p. 313-325.

8. Soto, I., et al., *Retinal ganglion cells downregulate gene expression and lose their axons within the optic nerve head in a mouse glaucoma model.* Journal of Neuroscience, 2008. **28**(2): p. 548-561.

9. Buckingham, B.P., et al., *Progressive ganglion cell degeneration precedes neuronal loss in a mouse model of glaucoma.* Journal of Neuroscience, 2008. **28**(11): p. 2735-2744.

10. Stowell, C., et al., *Retinal proteomic changes following unilateral optic nerve transection and early experimental glaucoma in non-human primate eyes.* Experimental Eye Research, 2011. **93**(1): p. 13-28.

11. Anders, F., et al., *Proteomic profiling reveals crucial retinal protein alterations in the early phase of an experimental glaucoma model.* Graefe's Archive for Clinical and Experimental Ophthalmology, 2017. **255**(7): p. 1395-1407.

12. Mirzaei, M., et al., *Retinal proteomics of experimental glaucoma model reveal intraocular pressure-induced mediators of neurodegenerative changes.* Journal of cellular biochemistry, 2020. **121**(12): p. 4931-4944.

13. Davis, C.-h.O., et al., *Transcellular degradation of axonal mitochondria.* Proceedings of the National Academy of Sciences, 2014. **111**(26): p. 9633-9638.

14. Sun, D., et al., *The morphology and spatial arrangement of astrocytes in the optic nerve head of the mouse.* Journal of Comparative Neurology, 2009. **516**(1): p. 1-19.

15. Jeon, C.-J., E. Strettoi, and R.H. Masland, *The major cell populations of the mouse retina.* Journal of Neuroscience, 1998. **18**(21): p. 8936-8946.

16. Masland, R.H., *The neuronal organization of the retina.* Neuron, 2012. **76**(2): p. 266-280.

17. Smith, C.A. and B.C. Chauhan, *Imaging retinal ganglion cells: enabling experimental technology for clinical application.* Progress in retinal and eye research, 2015. **44**: p. 1-14.

18. Sadun, A., *The afferent visual system: Anatomy and Physiology.* Ophthalmology, 2nd ed. Ed, Yanoff M, Duker JS. Mosby, St. Louis, 2004. **186**.

19. Ogden, T.E., *Nerve fiber layer of the owl monkey retina: retinotopic organization.* Investigative Ophthalmology & Visual Science, 1983. **24**(3): p. 265-269.

20. Mac Grory, B., et al., *Management of central retinal artery occlusion: a scientific statement from the American Heart Association.* Stroke, 2021. **52**(6): p. e282-e294.

21. Hernandez, M.R., F. Igoe, and A.H. Neufeld, *Cell culture of the human lamina cribrosa.* Investigative ophthalmology & visual science, 1988. **29**(1): p. 78-89.

22. Lozano, D.C., et al., *Early optic nerve head glial proliferation and Jak-Stat pathway activation in chronic experimental glaucoma.* Investigative ophthalmology & visual science, 2019. **60**(4): p. 921-932.

23. Hernandez, M.R., *The optic nerve head in glaucoma: role of astrocytes in tissue remodeling.* Progress in retinal and eye research, 2000. **19**(3): p. 297-321.

24. Kirwan, R.P., et al., *Effect of cyclical mechanical stretch and exogenous transforming growth factor-β1 on matrix metalloproteinase-2 activity in lamina cribrosa cells from the human optic nerve head.* Journal of glaucoma, 2004. **13**(4): p. 327-334.

25. Lambert, W., et al., *Neurotrophin and neurotrophin receptor expression by cells of the human lamina cribrosa.* Investigative ophthalmology & visual science, 2001. **42**(10): p. 2315-2323.

26. Mackenzie, P.J. and G.A. Cioffi, *Vascular anatomy of the optic nerve head.* Canadian Journal of Ophthalmology, 2008. **43**(3): p. 308-312.

27. Anderson, D.R., *Ultrastructure of human and monkey lamina cribrosa and optic nerve head.* Archives of Ophthalmology, 1969. **82**(6): p. 800-814.

28. Ffrench-Constant, C., et al., *Evidence that migratory oligodendrocyte-type-2 astrocyte (O-2A) progenitor cells are kept out of the rat retina by a barrier at the eye-end of the optic nerve.* Journal of neurocytology, 1988. **17**(1): p. 13-25.

29. Elkington, A., et al., *The structure of the lamina cribrosa of the human eye: an immunocytochemical and electron microscopical study.* Eye, 1990. **4**(1): p. 42-57.

30. Ye, H. and M.R. Hernandez, *Heterogeneity of astrocytes in human optic nerve head.* Journal of Comparative Neurology, 1995. **362**(4): p. 441-452.

31. Liu, B., et al., *Epidermal growth factor receptor activation: an upstream signal for transition of quiescent astrocytes into reactive astrocytes after neural injury.* Journal of Neuroscience, 2006. **26**(28): p. 7532-7540.

32. Yuan, L. and A.H. Neufeld, *Activated microglia in the human glaucomatous optic nerve head.* Journal of neuroscience research, 2001. **64**(5): p. 523-532.

33. Yazdankhah, M., et al., *Role of glia in optic nerve.* Progress in Retinal and eye Research, 2021. **81**: p. 100886.

34. Zamanian, J.L., et al., *Genomic analysis of reactive astrogliosis.* Journal of neuroscience, 2012. **32**(18): p. 6391-6410.

35. Anderson, M.A., et al., *Astrocyte scar formation aids central nervous system axon regeneration.* Nature, 2016. **532**(7598): p. 195-200.

36. Liddelow, S.A., et al., *Neurotoxic reactive astrocytes are induced by activated microglia.* Nature, 2017. **541**(7638): p. 481-487.

37. Klein, R.S. and C.A. Hunter, *Protective and pathological immunity during central nervous system infections.* Immunity, 2017. **46**(6): p. 891-909.

38. Crotti, A. and R.M. Ransohoff, *Microglial physiology and pathophysiology: insights from genome-wide transcriptional profiling.* Immunity, 2016. **44**(3): p. 505-515.

39. Golgi, C., *Contribuzione alla fina anatomia degli organi centrali del sistema nervoso*. 1871: Tipi Fava e Garagnani.

40. Selvam, S., T. Kumar, and M. Fruttiger, *Retinal vasculature development in health and disease.* Progress in retinal and eye research, 2018. **63**: p. 1-19.

41. Mosser, D.M. and J.P. Edwards, *Exploring the full spectrum of macrophage activation.* Nature reviews immunology, 2008. **8**(12): p. 958-969.

42. Kajihara, H., et al., *Activated astrocytes with glycogen accumulation in ischemic penumbra during the early stage of brain infarction: immunohistochemical and electron microscopic studies.* Brain research, 2001. **909**(1-2): p. 92-101.

43. Giordano, G., T.J. Kavanagh, and L.G. Costa, *Mouse cerebellar astrocytes protect cerebellar granule neurons against toxicity of the polybrominated diphenyl ether (PBDE) mixture DE-71.* Neurotoxicology, 2009. **30**(2): p. 326-329.

44. Chung, W.-S., et al., *Astrocytes mediate synapse elimination through MEGF10 and MERTK pathways.* Nature, 2013. **504**(7480): p. 394-400.

45. Tezel, G., *The role of glia, mitochondria, and the immune system in glaucoma.* Investigative ophthalmology & visual science, 2009. **50**(3): p. 1001-1012.

46. Perry, V.H., P.-B. Andersson, and S. Gordon, *Macrophages and inflammation in the central nervous system.* Trends in neurosciences, 1993. **16**(7): p. 268-273.

47. Raivich, G., et al., *Neuroglial activation repertoire in the injured brain: graded response, molecular mechanisms and cues to physiological function.* Brain research reviews, 1999. **30**(1): p. 77-105.

48. Perry, V.H., et al., *Inflammation in the nervous system.* Current opinion in neurobiology, 1995. **5**(5): p. 636-641.

49. Streit, W.J., S.A. Walter, and N.A. Pennell, *Reactive microgliosis.* Progress in neurobiology, 1999. **57**(6): p. 563-581.

50. Hanisch, U.-K. and H. Kettenmann, *Microglia: active sensor and versatile effector cells in the normal and pathologic brain.* Nature neuroscience, 2007. **10**(11): p. 1387-1394.

51. Yan, P., et al., *Matrix metalloproteinase-9 degrades amyloid-β fibrils in vitro and compact plaques in situ.* Journal of Biological Chemistry, 2006. **281**(34): p. 24566-24574.

52. Iwata, N., et al., *Metabolic regulation of brain Aβ by neprilysin.* Science, 2001. **292**(5521): p. 1550-1552.

53. Qiu, W.Q., et al., *Insulin-degrading enzyme regulates extracellular levels of amyloid β-protein by degradation.* Journal of Biological Chemistry, 1998. **273**(49): p. 32730-32738.

54. Reichert, F. and S. Rotshenker, *Complement-receptor-3 and scavenger-receptor-AI/II mediated myelin phagocytosis in microglia and macrophages.* Neurobiology of disease, 2003. **12**(1): p. 65-72.

55. Makranz, C., et al., *Phosphatidylinositol 3-kinase, phosphoinositide-specific phospholipase-Cγ and protein kinase-C signal myelin phagocytosis mediated by complement receptor-3 alone and combined with scavenger receptor-AI/II in macrophages.* Neurobiology of disease, 2004. **15**(2): p. 279-286.

56. Heuss, N.D., et al., *Optic nerve as a source of activated retinal microglia post-injury.* Acta neuropathologica communications, 2018. **6**(1): p. 1-19.

57. Barron, K.D., *The microglial cell. A historical review.* Journal of the neurological sciences, 1995. **134**: p. 57-68.

58. Neufeld, A.H., *Microglia in the optic nerve head and the region of parapapillary chorioretinal atrophy in glaucoma.* Archives of ophthalmology, 1999. **117**(8): p. 1050-1056.

59. Tribble, J.R., et al., *Suppression of homeostatic gene expression and increased expression of metabolism-related genes are early features of glaucoma in optic nerve head microglia.* Biorxiv, 2019: p. 856427.

60. Wang, J.-W., et al., *Retinal microglia in glaucoma.* Journal of glaucoma, 2016. **25**(5): p. 459-465.

61. Madeira, M.H., et al., *Contribution of microglia-mediated neuroinflammation to retinal degenerative diseases.* Mediators of inflammation, 2015. **2015**.

62. Mac Nair, C.E., et al., *Tumor necrosis factor alpha has an early protective effect on retinal ganglion cells after optic nerve crush.* Journal of neuroinflammation, 2014. **11**(1): p. 1-14.

63. Paschalis, E.I., et al., *Microglia regulate neuroglia remodeling in various ocular and retinal injuries.* The Journal of Immunology, 2019. **202**(2): p. 539-549.

64. Diem, R., et al., *Reduction of potassium currents and phosphatidylinositol 3-kinase-dependent AKT phosphorylation by tumor necrosis factor-α rescues axotomized retinal ganglion cells from retrograde cell death in vivo.* Journal of Neuroscience, 2001. **21**(6): p. 2058-2066.

65. Evans, L.P., et al., *Modulation of post-traumatic immune response using the IL-1 receptor antagonist anakinra for improved visual outcomes.* Journal of neurotrauma, 2020. **37**(12): p. 1463-1480.

66. Tezel, G. and M.B. Wax, *Increased production of tumor necrosis factor-α by glial cells exposed to simulated ischemia or elevated hydrostatic pressure induces apoptosis in cocultured retinal ganglion cells.* Journal of Neuroscience, 2000. **20**(23): p. 8693-8700.

67. Roh, M., et al., *Etanercept, a widely used inhibitor of tumor necrosis factor-α (TNF-α), prevents retinal ganglion cell loss in a rat model of glaucoma.* PloS one, 2012. **7**(7): p. e40065.

68. Bosco, A., et al., *Reduced retina microglial activation and improved optic nerve integrity with minocycline treatment in the DBA/2J mouse model of glaucoma.* Investigative ophthalmology & visual science, 2008. **49**(4): p. 1437-1446.

69. Baptiste, D., et al., *Effects of minocycline and tetracycline on retinal ganglion cell survival after axotomy.* Neuroscience, 2005. **134**(2): p. 575-582.

70. Levkovitch-Verbin, H., et al., *Minocycline delays death of retinal ganglion cells in experimental glaucoma and after optic nerve transection.* Archives of ophthalmology, 2006. **124**(4): p. 520-526.

71. Shimazawa, M., et al., *Neuroprotective effects of minocycline against in vitro and in vivo retinal ganglion cell damage.* Brain research, 2005. **1053**(1-2): p. 185-194.

72. Karlstetter, M., S. Ebert, and T. Langmann, *Microglia in the healthy and degenerating retina: insights from novel mouse models.* Immunobiology, 2010. **215**(9-10): p. 685-691.

73. Hilla, A.M., H. Diekmann, and D. Fischer, *Microglia are irrelevant for neuronal degeneration and axon regeneration after acute injury.* Journal of Neuroscience, 2017. **37**(25): p. 6113-6124.

74. Joshi, A.U., et al., *Fragmented mitochondria released from microglia trigger A1 astrocytic response and propagate inflammatory neurodegeneration.* Nature neuroscience, 2019. **22**(10): p. 1635-1648.

75. Zhang, N., et al., *Prevalence of primary open angle glaucoma in the last 20 years: a meta-analysis and systematic review.* Scientific Reports, 2021. **11**(1): p. 1-12.

76. Quigley, H.A., *Open-angle glaucoma.* New England Journal of Medicine, 1993. **328**(15): p. 1097-1106.

77. Shields, M., et al., *Classification of the glaucoma.* The glaucomas, 1996: p. 717-725.

78. Lee, S., et al., *Mitochondrial dysfunction in glaucoma and emerging bioenergetic therapies.* Experimental eye research, 2011. **93**(2): p. 204-212.

79. Clement, C.I., S. Bhartiya, and T. Shaarawy, *New perspectives on target intraocular pressure.* Survey of ophthalmology, 2014. **59**(6): p. 615-626.

80. Klein, B.E., et al., *Prevalence of glaucoma: the Beaver Dam eye study.* Ophthalmology, 1992. **99**(10): p. 1499-1504.

81. Sommer, A., *Intraocular pressure and glaucoma.* Am J Ophthalmol, 1989. **107**: p. 186-188.

82. Lichter, P.R., *Impact of intraocular pressure reduction on glaucoma progression.* JAMA, 2002. **288**(20): p. 2607-2608.

83. Zhu, Y., et al., *Ultrastructural morphology of the optic nerve head in aged and glaucomatous mice.* Investigative ophthalmology & visual science, 2018. **59**(10): p. 3984-3996.

84. Baltan, S., et al., *Metabolic vulnerability disposes retinal ganglion cell axons to dysfunction in a model of glaucomatous degeneration.* Journal of Neuroscience, 2010. **30**(16): p. 5644-5652.

85. Cooper, M.L., et al., *Early astrocyte redistribution in the optic nerve precedes axonopathy in the DBA/2J mouse model of glaucoma.* Experimental eye research, 2016. **150**: p. 22-33.

86. Coughlin, L., et al., *Mitochondrial morphology differences and mitophagy deficit in murine glaucomatous optic nerve.* Investigative ophthalmology & visual science, 2015. **56**(3): p. 1437-1446.

87. Williams, P.A., et al., *Vitamin B3 modulates mitochondrial vulnerability and prevents glaucoma in aged mice.* Science, 2017. **355**(6326): p. 756-760.

88. Hernandez, M.R., et al., *Age-related changes in the extracellular matrix of the human optic nerve head.* American journal of ophthalmology, 1989. **107**(5): p. 476-484.

89. Albon, J., et al., *Age related compliance of the lamina cribrosa in human eyes.* British Journal of Ophthalmology, 2000. **84**(3): p. 318-323.

90. Girard, M.J., et al., *Scleral biomechanics in the aging monkey eye.* Investigative ophthalmology & visual science, 2009. **50**(11): p. 5226-5237.

91. Coudrillier, B., et al., *Effects of age and diabetes on scleral stiffness.* Journal of biomechanical engineering, 2015. **137**(7).

92. Coudrillier, B., et al., *Effects of peripapillary scleral stiffening on the deformation of the lamina cribrosa.* Investigative ophthalmology & visual science, 2016. **57**(6): p. 2666-2677.

93. John, S., et al., *Essential iris atrophy, pigment dispersion, and glaucoma in DBA/2J mice.* Investigative ophthalmology & visual science, 1998. **39**(6): p. 951-962.

94. McKinnon, S.J., C.L. Schlamp, and R.W. Nickells, *Mouse models of retinal ganglion cell death and glaucoma.* Experimental eye research, 2009. **88**(4): p. 816-824.

95. Anderson, M.G., et al., *Mutations in genes encoding melanosomal proteins cause pigmentary glaucoma in DBA/2J mice.* Nature genetics, 2002. **30**(1): p. 81-85.

96. Howell, G.R., et al., *Absence of glaucoma in DBA/2J mice homozygous for wild-type versions of Gpnmb and Tyrp1.* BMC genetics, 2007. **8**(1): p. 1-10.

97. Libby, R.T., et al., *Inherited glaucoma in DBA/2J mice: pertinent disease features for studying the neurodegeneration.* Visual neuroscience, 2005. **22**(5): p. 637-648.

98. Morgan, J.E. and J.R. Tribble, *Microbead models in glaucoma.* Experimental eye research, 2015. **141**: p. 9-14.

99. Johnson, T.V. and S.I. Tomarev, *Rodent models of glaucoma.* Brain research bulletin, 2010. **81**(2-3): p. 349-358.

100. Wilkison, S.J., et al., *Local Accumulation of Axonal Mitochondria in the Optic Nerve Glial Lamina Precedes Myelination.* Frontiers in neuroanatomy, 2021. **15**.

101. Fiedorowicz, M., et al., *Tryptophan pathway abnormalities in a murine model of hereditary glaucoma.* International Journal of Molecular Sciences, 2021. **22**(3): p. 1039.

102. Lin, J.Q., F.W. van Tartwijk, and C.E. Holt, *Axonal mRNA translation in neurological disorders.* RNA biology, 2021. **18**(7): p. 936-961.

103. Koppers, M., et al., *Receptor-specific interactome as a hub for rapid cue-induced selective translation in axons.* Elife, 2019. **8**: p. e48718.

104. Nijssen, J., et al., *Axon-seq decodes the motor axon transcriptome and its modulation in response to ALS.* Stem cell reports, 2018. **11**(6): p. 1565-1578.

105. Shigeoka, T., et al., *Dynamic axonal translation in developing and mature visual circuits.* Cell, 2016. **166**(1): p. 181-192.

106. Martin, K.C. and A. Ephrussi, *mRNA localization: gene expression in the spatial dimension.* Cell, 2009. **136**(4): p. 719-730.

107. Holt, C.E. and E.M. Schuman, *The central dogma decentralized: new perspectives on RNA function and local translation in neurons.* Neuron, 2013. **80**(3): p. 648-657.

108. Terenzio, M., G. Schiavo, and M. Fainzilber, *Compartmentalized signaling in neurons: from cell biology to neuroscience.* Neuron, 2017. **96**(3): p. 667-679.

109. Spillane, M., et al., *Mitochondria coordinate sites of axon branching through localized intra-axonal protein synthesis.* Cell reports, 2013. **5**(6): p. 1564-1575.

110. Minckler, D., I. McLean, and M. Tso, *Distribution of axonal and glial elements in the rhesus optic nerve head studied by electron microscopy.* American journal of ophthalmology, 1976. **82**(2): p. 179-187.

111. Andrews, R.M., et al., *Histochemical localisation of mitochondrial enzyme activity in human optic nerve and retina.* British Journal of Ophthalmology, 1999. **83**(2): p. 231-235.

112. Bristow, E.A., et al., *The distribution of mitochondrial activity in relation to optic nerve structure.* Archives of ophthalmology, 2002. **120**(6): p. 791-796.

113. Hollander, H., et al., *Evidence of constriction of optic nerve axons at the lamina cribrosa in the normotensive eye in humans and other mammals.* Ophthalmic research, 1995. **27**(5): p. 296-309.

114. Minckler, D.S., A.H. Bunt, and I.B. Klock, *Radioautographic and cytochemical ultrastructural studies of axoplasmic transport in the monkey optic nerve head.* Investigative ophthalmology & visual science, 1978. **17**(1): p. 33-50.

115. Mutsaers, S. and W. Carroll, *Focal accumulation of intra-axonal mitochondria in demyelination of the cat optic nerve.* Acta neuropathologica, 1998. **96**(2): p. 139-143.

116. Man, C.Y.W., P. Chinnery, and P. Griffiths, *Optic neuropathies–importance of spatial distribution of mitochondria as well as function.* Medical hypotheses, 2005. **65**(6): p. 1038-1042.

117. Yu, D.-Y., et al., *Retinal ganglion cells: energetics, compartmentation, axonal transport, cytoskeletons and vulnerability.* Progress in retinal and eye research, 2013. **36**: p. 217-246.

118. Gaal, T., et al., *Transcription regulation by initiating NTP concentration: rRNA synthesis in bacteria.* Science, 1997. **278**(5346): p. 2092-2097.

119. Schneider, D.A., T. Gaal, and R.L. Gourse, *NTP-sensing by rRNA promoters in Escherichia coli is direct.* Proceedings of the National Academy of Sciences, 2002. **99**(13): p. 8602-8607.

120. Cioni, J.-M., et al., *Late endosomes act as mRNA translation platforms and sustain mitochondria in axons.* Cell, 2019. **176**(1-2): p. 56-72. e15.

121. Gale, J.R., et al., *Nuclear-encoded mitochondrial mRNAs: a powerful force in axonal growth and development.* The Neuroscientist, 2018. **24**(2): p. 142-155.

122. Kaplan, B.B., et al., *Axonal protein synthesis and the regulation of local mitochondrial function.* Cell biology of the axon, 2009: p. 1-25.

123. Yoon, B.C., et al., *Local translation of extranuclear lamin B promotes axon maintenance.* Cell, 2012. **148**(4): p. 752-764.

124. Dielemans, I., et al., *The prevalence of primary open-angle glaucoma in a population-based study in the Netherlands: the Rotterdam Study.* Ophthalmology, 1994. **101**(11): p. 1851-1855.

125. Kahn, H.A. and R.C. Milton, *Alternative definitions of open-angle glaucoma: effect on prevalence and associations in the Framingham Eye Study.* Archives of ophthalmology, 1980. **98**(12): p. 2172-2177.

126. Mitchell, P., et al., *Prevalence of open-angle glaucoma in Australia: the Blue Mountains Eye Study.* Ophthalmology, 1996. **103**(10): p. 1661-1669.

127. Leske, M.C., et al., *Risk factors for open-angle glaucoma: the Barbados Eye Study.* Archives of ophthalmology, 1995. **113**(7): p. 918-924.

128. Wong, A.A. and R.E. Brown, *A neurobehavioral analysis of the prevention of visual impairment in the DBA/2J mouse model of glaucoma.* Investigative ophthalmology & visual science, 2012. **53**(9): p. 5956-5966.

Biography

Zollie Yavarow was born and raised in Massachusetts. Taking an interest in science from an early age, Zollie studied Biochemistry in college, graduating from Mount Holyoke College in South Hadley, Massachusetts in 2017. During this time, she completed independent research on the lysosomal storage disease Sialidosis, a rare genetic disorder. Zollie moved to Durham, North Carolina to start her PhD in the Cell and Molecular Biology umbrella program at Duke University, later declaring her degree in Pharmacology. After exploring rotations in breast cancer, bone cancer, and the *drosophila* hindgut, she continued research on rare genetics conditions studying Glycogen Storage Disease Type Ia in the lab of Dr. Dwight Koeberl. Zollie later transitioned to the lab of Dr. Romain Cartoni studying the optic nerve and glaucoma. Through her study of disease, she developed an interest in health care equity and advanced therapeutics, leading her to pursue a concurrent master's degree in Bioethics and Science Policy. Zollie lives in Durham, NC with her partner and two dogs and has enjoyed watching Durham grow. She unwinds by exploring North Carolina, visiting grocery stores and restaurants, and hosting game nights.